J. Membrane Biol. 136, 31–42 (1993)

The Journal of
Membrane
Biology

Properties of Acetylcholine Receptors in Adult Rat Skeletal Muscle Fibers in Culture

Fabio Grohovaz[2], Paola Lorenzon[1], Fabio Ruzzier[1], Robert Zorec[3]

[1]Institute of Physiology, University of Trieste, via A. Fleming 22, I-34127 Trieste, Italy
[2]C.N.R. Center of Cytopharmacology and Center B. Ceccarelli, DIBIT, S. Raffaele Institute, 20132 Milano, Italy
[3]Institute of Pathophysiology, University of Ljubljana, 61105 Ljubljana, Slovenia

Received: 27 January 1993/Revised: 10 May 1993

Abstract. The distribution and biophysical properties of acetylcholine receptors were studied, using morphological and patch-clamp techniques, in adult rat skeletal muscle fibers dissociated by collagenase and maintained in culture. Up to ten hours after dissociation, there were no changes in either the distribution or the biophysical properties of junctional acetylcholine receptors. In long-term culture (5 to 14 days), a new type of acetylcholine receptor was inserted all over the muscle fibers; the channel properties were characterized by a longer open time and a smaller conductance, similar to what has been observed in in vivo denervated muscles. Using autoradiography, we found that during culture an impaired incorporation of new acetylcholine receptors in the former endplates caused a progressive decrease in the density of junctional acetylcholine receptors. This contrasts with muscle fibers denervated in vivo, where the density of receptors does not change after denervation.

Key words: Acetylcholine channels — Denervation — Patch clamp — Videoimaging

Introduction

There is compelling evidence that the distribution and biophysical properties of acetylcholine receptors (AChRs) in skeletal muscle fibers change following denervation. In particular, the AChR channels exhibit longer open time and smaller conductance and this is accompanied by their appearance along the whole fiber length, as indicated by electrophysiological studies and α-bungarotoxin (αBTx) binding (Axelsson & Thesleff, 1959; Miledi, 1960*a*; Fambrough, 1979; Schuetze & Role, 1987; Steinbach, 1989). Three main mechanisms have been suggested to account for these changes: first, the existence of trophic substances, involved in the control of the phenotypic expression of the AChRs (Miledi, 1960*a*, *b*; Gutmann, 1976; McArdle, 1983); second, the inactivity of the muscle fibers, following removal of the nerve input (Lømo & Rosenthal, 1972); and third, nerve breakdown products, as important for the initiation and control of the denervation phenomena (Cangiano, 1985). Because of this complexity, it would be of great importance to have a preparation of muscle fibers in an adequately controlled environment, in which postdenervation phenomena could be expressed. A preparation that meets this end is the suspension of adult muscle fibers (Bekoff & Betz, 1977). However, apart from a few previous works (Cull-Candy, Miledi & Uchitel, 1982*a*, *b*), the supersensitivity of ACh response and the biophysical properties of long-term cultured adult muscle fibers have not been studied in detail. We have therefore investigated the appearance of the postdenervation changes of AChR in enzymatically dissociated skeletal muscle fibers maintained in cell culture without previous denervation in vivo, and we denote this procedure as denervation in vitro.

We have monitored the ACh-activated channel properties and their distribution by electrophysiological and morphological methods in freshly dispersed and cultured muscle fibers. After culturing muscle fibers for a few days, the ACh-activated channels acquire, in fact, properties that are described for the denervation in vivo. In contrast, under such conditions, we show that the density of

Correspondence to: F. Ruzzier

AChR accumulation is different to that observed in vivo. Preliminary accounts of some of this work have been given previously (Ruzzier & Grohovaz, 1986; Ruzzier & Zorec, 1988; Ruzzier et al., 1991).

Materials and Methods

Cell Culture

Experiments were carried out on male Wistar rats (100–200 g), killed by anesthetic overdose. Single muscle fibers were obtained from the *M. flexor digitorum brevis*, a fast-twitch skeletal muscle from the rear feet, according to a modification of the method of Bekoff & Betz (1977). Briefly, the muscles were dissected from the animal and placed in 35 mm Sterilin tissue culture dishes, in 3 ml Eagle's Minimal Essential Medium (EMEM; Flow, UK) supplemented with horse serum (5% by volume; Flow), penicillin (100 U/ml), streptomycin (100 μg/ml) and 2 mM L-glutamine. To this medium, collagenase (Type 1, Sigma, St. Louis, MO; later on, Boehringer Mannheim, Germany) was added (3 mg/ml). No apparent differences of electrophysiological and morphological results were observed with the two commercial types of collagenase used. The muscles were incubated for 3 hr at 37°C in an air-5% CO_2 incubator at 100% humidity, then washed in fresh EMEM and mechanically dissociated into single muscle fibers by repeated passages through Pasteur pipettes whose tips had been fire-polished to produce openings of successively decreasing size. The isolated muscle fibers were then cultured at 37°C in plastic dishes for up to 2 weeks.

Autoradiography

Dissociated fibers to be labeled with iodinated αBTx were washed in a mammalian Ringer solution containing (mM): NaCl 117, KCl 5.4, $CaCl_2$ 1.8, $MgSO_4$ 0.8, NaH_2PO_4 1, glucose 5.5, HEPES buffer 10, adjusted to pH 7.3 by addition of NaOH. Fibers were subsequently incubated for 3 hr at 4°C, to avoid internalization processes, in a Ringer solution containing 2 μg/ml [^{125}I]αBTx (10–20 μCi/μg; New England Nuclear, Boston, MA) and 5 mg/ml bovine serum albumin (BSA; Sigma). After the incubation, the unbound toxin was removed by several washes with the Ringer solution, and Trypan blue (0.4 mg/ml; Sigma) was added in order to distinguish viable cells. Fibers were fixed for 1 hr at room temperature with 2% glutaraldehyde/2% formaldehyde (freshly prepared from paraformaldehyde) in 0.1 M sodium phosphate buffer, pH 7.3, washed with 0.1 M sodium phosphate buffer, pH 7.3, and finally suspended in double distilled water. A thin layer of the suspension was laid on glass slides previously coated with a formvar film. The slides were air-dried, dipped in NTB-2 emulsion (Eastman Kodak, Rochester, NY) at 45°C and exposed in the dark in dessicator boxes. Autoradiograms were developed at 21°C in D19 for 2 min, rinsed in water and then fixed in F5. Slides were washed in water, air-dried and observed with a dark field illumination in a Photomicroscope III (Zeiss, Milan, Italy).

Immunocytochemistry

For immunostaining of AChRs, dissociated fibers were maintained in culture for two hours, washed with Ringer and incubated for 3 hr at 4°C in a Ringer solution containing 2 μg/ml of highly purified αBTx (kindly provided by Dr. C. Gotti, CNR Ctr. Cytopharmacology, Milan, Italy) and 5 mg/ml BSA (Sigma). After 1 hr fixation with 1% formaldehyde in 0.1 M sodium phosphate buffer, pH 7.3, the immunostaining was performed by an indirect procedure. After extensive washes in 0.1 M glycine-NaOH, pH 7.3, and 0.1 M sodium phosphate buffer, pH 7.3, fibers were incubated for 1 hr with rabbit anti-αBTx purified antibodies (kindly provided by Dr. C. Gotti), diluted 1 : 100 in a solution of 5 mg/ml of BSA in 0.1 M PBS (phosphate-buffered saline), pH 7.3 (BSA-PBS). Fibers were then processed at room temperature according to one of the two following schedules. (A) Light microscopy: (1) 4 washes in BSA-PBS; (2) incubation with anti-rabbit, biotinylated species-specific whole antibodies (Amersham International, Amersham, UK) dilutes 1 : 100 in BSA-PBS; (3) 4 washes in BSA-PBS; (4) incubation for 1 hr with Texas Red-streptavidin (Amersham) diluted 1 : 150 in BSA-PBS; (5) 4 washes in BSA-PBS. Single muscle fibers were mounted, under a dissecting microscope, on glass slides in 95% (vol/vol) glycerol. (B) Electron microscopy: (1) 4 washes in BSA-PBS; (2) incubation with protein A-colloidal gold conjugated; (3) postfixation with 2% OsO_4 in 0.1 M sodium phosphate buffer, pH 7.3; (4) 4 washes in 0.1 M sodium phosphate buffer, pH 7.3. Single muscle fibers were subsequently processed for electron microscopy according to standard procedures. Silver-gray sections were cut with a diamond knife (Diatome, Bienne, Switzerland) on a Reichert-Jung Ultracut microtome (Reichert, Wien, Austria), and examined with a H-600 Hitachi electron microscope (Hitachi, Tokyo, Japan).

Videoimaging

Muscle fibers were exposed to tetramethylrhodamine-αBTx during or immediately after enzymatic dissociation, washed in mammalian Ringer solution and transferred on the heating stage of an inverted microscope (IM 35, Zeiss). Excitation light (50 W, Hg arc lamp) was reduced to 10% by inserting neutral density filters to preserve the long-term viability of fibers. Fluorescence images were collected by a highly sensitive Intensifier Silicon-Intensifier Target tube camera (2400-09, Hamamatsu Photonics, Japan) and fed into a videoprocessor (Argus 100, Hamamatsu). To improve the signal to noise ratio of the images, 32 frames were averaged each time. Background images were similarly obtained in out of focus condition, stored into a frame memory and then subtracted to obtain the final images. The excitation light was controlled by a shutter, operated by Argus 100, to reduce the light exposure of the fibers to the time strictly needed for image acquisition. Two trains of five averaged images were collected, in rapid sequence, immediately after dissociation and 6 hr later, respectively. Images from the same train showed highly consistent values of fluorescence intensity, with no signs of definite trends, indicating negligible photobleaching, while images from the two trains were significantly different.

Freeze Drying

Dissociated muscle fibers were fixed with 2% glutaraldehyde/2% formaldehyde in 0.1 M sodium phosphate buffer, pH 7.3, at 4°C. After several washes in 0.1 M sodium phosphate buffer, the fibers were dehydrated through a graded series of methanol at 4°C, laid onto low mass specimen carriers and rapidly frozen into a mixture of 75% propane and 25% isopentane cooled at −196°C (Jehl et al., 1981). The frozen specimens were transferred under liquid

nitrogen to a specially designed table and placed in a Cryofract 190 freeze-fracture apparatus (Reichert Jung, Paris, France). The temperature was raised slowly from −130 to −50°C to maintain the vacuum at values better than $1 \cdot 10^{-8}$ Torr. The total pressure and the water partial pressure were monitored by a quadrupole mass spectrometer (Anavac 2, VG Gas Analysis, Winsford, UK); when they reached a plateau at −50°C, the temperature was lowered to −100°C and the specimen was shadowed without previous fracture. The platinum-carbon replicas were examined with an H-600 Hitachi electron microscope.

Single-Channel Recording

Experiments were performed in mammalian Ringer at room temperature (20–25°C) under phase contrast illumination using a Zeiss IM 35 inverted microscope and objectives 2.5, 16 and 40×. Recording pipettes were pulled from borosilicate capillaries (GC120F, Clark Electromedical Instruments, Reading, UK) on a modified vertical puller (Scientific & Research Instruments, UK) and heat-polished according to the methods of Corey and Stevens (1983). Pipettes, with a tip diameter of about 1–2 μm (resistances in the range 10–20 MΩ) were filled with 100 to 200 nM ACh (Sigma) dissolved in the bath solution (mammalian Ringer). Gigaohm-seal, cell-attached patches were obtained with conventional techniques (Hamill et al., 1981) with a home-made amplifier (SWAM II, Slovenia; Henigman, Kordaš & Zorec, 1987) from synaptic and nonsynaptic patches of membrane.

The current signal from the amplifier was stored on a VHS video recorder following pulse code modulation (modified 501ES, Sony) for subsequent analysis. Signals were low-pass filtered at 3 kHz (−3dB, 4-pole Bessel) and connected to the analog-to-digital converter CED 1401 (Cambridge, UK), sampled at 10–20 kHz and stored on the computer hard disk (IBM PC compatible). Acquisition and analysis software was kindly provided by Dr. J. Dempster (Strathclyde University, Glasgow, UK).

Single channel currents were analyzed with the program previously described (Dempster, 1989). The current amplitude distribution was determined to obtain the mean current amplitude value at different pipette potentials. Channel conductance was determined from the slope of the line obtained by linear regression or by estimation from the amplitude of the elementary currents and the driving potential which was taken to be equal to the pipette holding potential, assuming the reversal potential of 0 mV for ACh-activated channels (Ritchie & Fambrough, 1975; Hamill & Sakmann, 1981). The digitized record was reduced to a table of transition times and amplitudes by a routine of amplitude threshold analysis. The signal was scrolled until an amplitude greater than the threshold (30 to 50 % of mean elementary current amplitude) was detected. The apparent open time was defined as the duration of the event at one-third to one-half the mean amplitude current. A histogram was formed and an exponential distribution curve was fitted to the data, composed of one or the sum of two exponential functions. The minimum duration accepted in this analysis was 150 μsec (20 kHz sampling rate) and 300 μsec (10 kHz sampling rate). Additional conductance states were not taken into account in such elementary current kinetic analysis, as the probability of observing these states was typically less than 3% of all channel openings. The probability of occurrence of an elementary current conductance state was calculated for patches with at least 100 openings, as percentage of time spent in a particular state. In these estimates, the data from patches of membrane recorded at different holding potentials were pooled, as no apparent relationship was observed between the percentage of time spent in a particular conductance state and pipette potential. All the data, when possible, are given as mean ± SEM.

Abbreviations

ACh	acetylcholine
AChR	acetylcholine receptor
BSA	bovine serum albumin
αBTx	α-bungarotoxin
EMEM	Eagle's Minimal Essential Medium
PBS	phosphate-buffered saline

Results

Distribution of the AChRs

Freshly dissociated fibers presented a pattern of distribution of iodinated αBTx binding sites similar to that previously described for innervated muscle labeled in vivo (Hartzell & Fambrough, 1972). Viable fibers, as judged by the trypan blue exclusion test, showed a single heavy deposit of silver grain, usually in the proximity of the center of the fiber (Fig. 1*A*), indicating that extrajunctional AChRs were not detected (*see also* Ito et al., 1978).

When dissociated fibers were cultured for up to 14 days, the density of junctional AChRs progressively declined while extrajunctional AChRs increased, giving rise to a patchy or widespread distribution of silver grains (Fig. 1*B* and *C*).

Similar results were obtained by measuring the extrajunctional sensitivity to ionophoretic ACh application (*not shown; see also* Bekoff & Betz, 1977), and by AChR fluorescent staining. In the junctional area of freshly dissociated fibers, this technique revealed the presence of tightly packed branches (Fig. 1*D* and *E*). After two to six days in culture, this pattern was still recognizable, though with a more faint appearance (Fig. 1*F* and *G*). In addition, at later times, numerous discrete patches of fluorescence appeared extrajunctionally (Fig. 1*H*).

Properties of Single Channels Opened by ACh

Conductance

In freshly dissociated muscle fibers, the former endplate was easily identified, by phase-contrast microscopy, as an optically distinct roughness of the fiber surface. The ACh-induced channel activity was investigated along the muscle fiber by the patch-clamp technique in the cell-attached configuration. With 200 nM ACh in the pipette-filling solution, chan-

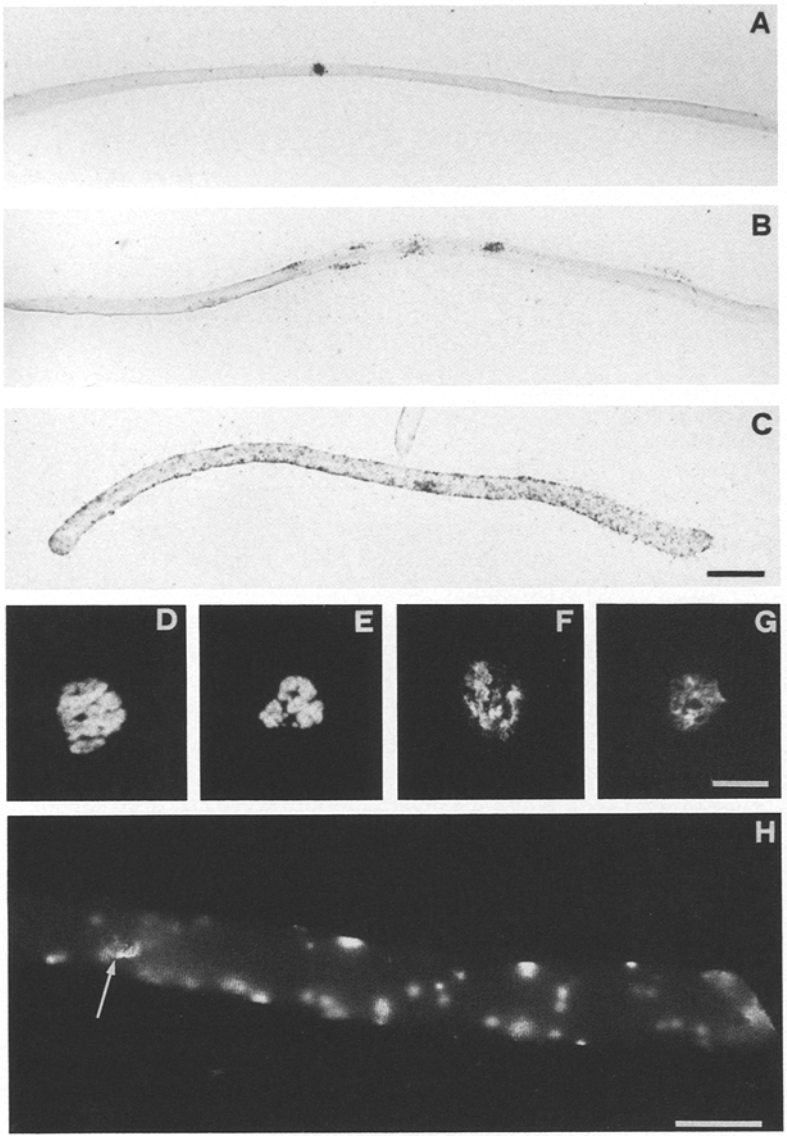

Fig. 1. AChR labeling in freshly dissociated and in long-time cultured muscle fibers. Autoradiographs of freshly dissociated (*A*) and 14-day cultured (*B* and *C*) fibers reveal that [^{125}I]αBTx binding sites are, initially, strictly confined in a small area while, at later times, they are distributed along the entire fiber with a patchy distribution. Fluorescent staining of the fibers was done by an indirect procedure (*see* Materials and Methods, Immunocytochemistry). The endplate area pattern is recognizable immediately after dissociation (*D* and *E*) as well as after 2 (*F*), 6 (*G*) and 14 (*H*, arrow) days in culture, although the fluorescent signal shows a progressive decrease. In addition, numerous discrete patches of fluorescent staining are evenly distributed on fibers maintained in long-term culture (*H*). Scale bar in *C*: 100 μm (*A–C*); bar in *G*: 20 μm (*D–G*); bar in *H*: 50 μm.

nel activity was found in membrane patches from neither the extrajunctional area (n = 15) nor the perijunctional area (n = 4), while one or two channels, as judged by the elementary current distribution, were present in patches from the junctional area (n = 7). The probability of simultaneously observing two events was typically around 0 to 2% of the duration of all elementary currents. The distributions of elementary currents were well fitted by Gaussian curves (Fig. 2). In some experiments, a slight skewness of the elementary current amplitude distribution of the open ACh-activated channel was observed. These humps in the shape of the distribution corresponded to additional class(es) of ACh-activated channels occurring with low probability (*see below*). Amplitudes of these events were measured manually by inspecting the whole record in which skewness of the elementary current amplitude distribution was observed (Fig. 2*B* and *C*). The major amplitude class of ACh-activated channels in freshly dissociated muscle fibers had a conductance of around 75 pS (Table, Fig. 2*A*). Openings to only this conductance state were recorded in three out of seven patches. In the other patches there were elementary current events with a lower conductance of 53.5 ± 4.7 pS (mean ± SEM, n = 4 patches). In three patches (out of seven), the time spent in the lower conductance state was around 1% of all conductance states, whereas in one patch it was around 9.5%, the rest being occupied by the 75 pS conductance state.

When muscle fibers were kept in culture from

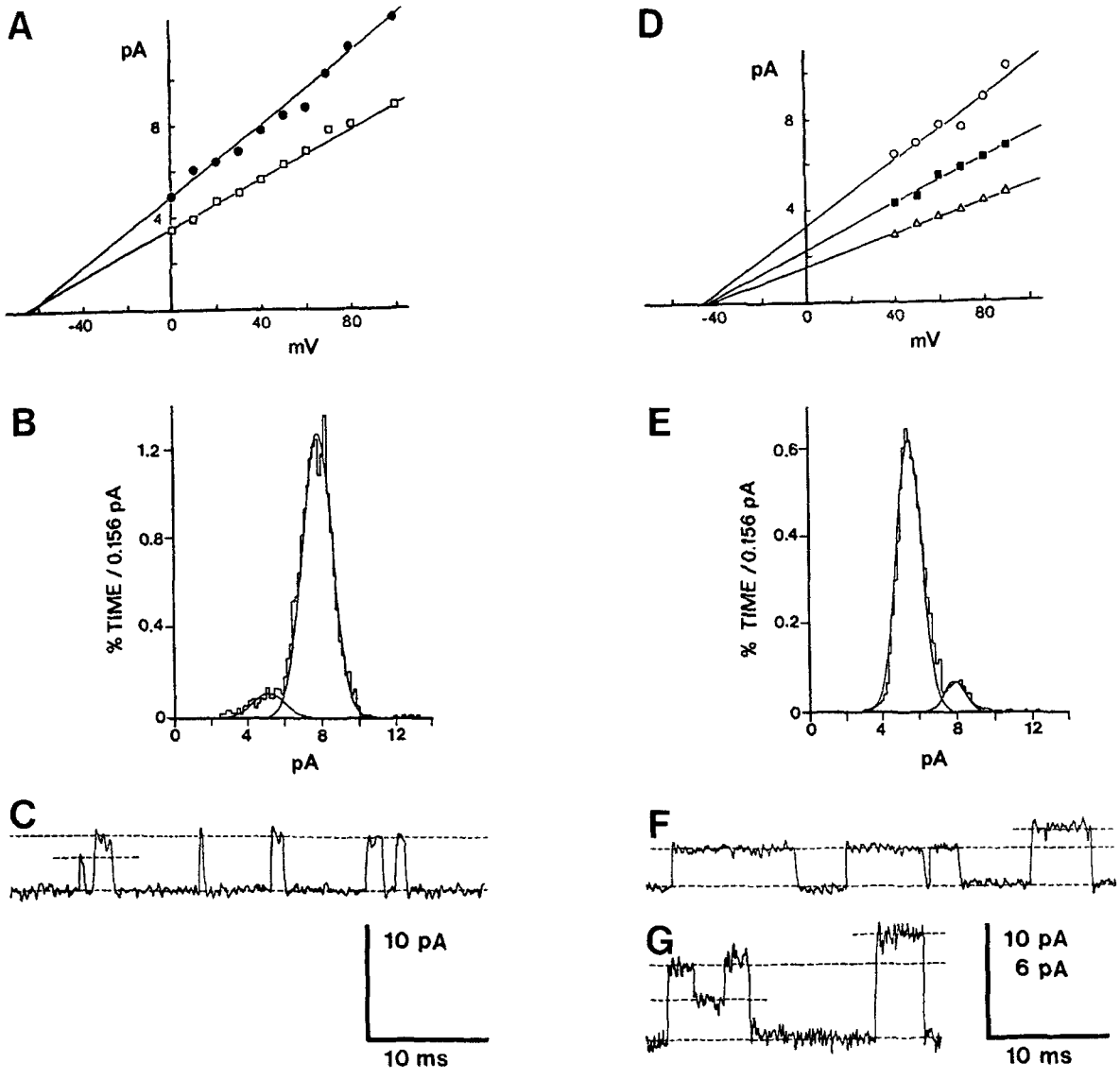

Fig. 2. ACh-activated channel properties. Amplitude classes of ACh-activated elementary currents in muscle fibers freshly dissociated (*A–C*) and cultured for 9 (*D–F*) and 6 days (*G*). *A*, and *D*, representative current *vs.* voltage plot for elementary currents. Filled symbols indicate the major conductance class of ACh-activated elementary currents, which were present for more than 90% of time spent in any conductance state. Lines were drawn by linear regression. *B* and *E* show two representative amplitude distributions for elementary currents recorded at 60 mV pipette potential (442 and 502 current events were respectively used to construct the distributions). Signals in all panels were acquired at 20 kHz and low-pass filtered (3 kHz, −3 dB, 4-pole, Bessel). In *B*, Gaussian curves were fitted with 7.78 ± 0.80 pA and 5.12 ± 0.82 pA (mean ± SD). The areas under the curves show that the larger amplitude class consisted of 1.65% of time of the record and that the lower amplitude class consisted of 0.14% of time of the record. In *E* the corresponding parameters were 5.50 ± 0.67 pA with an area of 6.65% of time of the record and 7.90 ± 0.55 pA with an area of 0.61% of time of the record. *C* shows typical current events with two amplitude classes in freshly dissociated muscle fibers (the same experiment as in *B*). *F* and *G* show typical amplitude elementary current classes in cultured muscle. Currents in *F* are from the same experiment as *E*. Trace in *G* is from a different patch. Note the three amplitude classes of which the lowest may form a subconductance state of the middle class, which was the most frequently observed, with a probability of more than 97% of time of the recording. Dashed lines in *C* and *F* are the means obtained in histograms *B* and *E*, respectively.

5 to 14 days, the phase-contrast identification of endplate area became more difficult. Channel activity was present in all regions of the fiber, as expected from the autoradiographic results described above, as well as from previous electrophysiological works.

The major amplitude class of single ACh-activated currents had a conductance of around 49 pS (*see* Table, Fig. 2*D*). Openings to this conductance state consisted of 75 to 98% (91 ± 4.5%, $n = 5$ patches) of the time spent in any conductance state. In addition,

there were openings to a higher conductance state of 68.5 ± 4.8 pS (Fig. 2*D-G*), which represented 4.9 ± 1.3% of time spent in any conductance state. A small conductance class of 26.9 ± 2.1 pS was also observed, which represented 5.1 ± 2.6% of the total. These openings may correspond to a subconductance state (Hamill & Sakmann, 1981; Auerbach & Sachs, 1984; Colquhoun & Sakmann, 1985; Henderson, Lechleiter & Brehm, 1987) since they were occasionally seen as openings to or from the major conductance state (Fig. 2*G*). Such events were not observed for the 68.5 pS conductance class of single ACh-activated channels. The conductances of all these classes of single channel amplitudes, in freshly dissociated and long-term cultured fibers, were independent of the length of time of recording.

Kinetic Properties

Average duration of elementary currents was estimated for all conductance states in a patch. In long-term cultured fibers the average channel apparent open time was about 3 times longer than in freshly dissociated muscle (*see* Table, and also Henderson et al., 1987; Cull-Candy et al., 1982*b*).

Mean apparent open channel duration depends on membrane potential. The voltage dependence in the form $t_{(V)} = t_o \cdot e^{(-V/H)}$ (Magleby & Stevens, 1972; Kordaš & Zorec, 1984; Mishina et al., 1986) was thus fitted to the data, where t equals the average apparent open channel duration, t_o is the average apparent open channel duration at 0 mV, V is potential in mV, and H represents the shift in membrane potential that causes an e-fold change in the mean open channel duration. It appeared that in the long-term culture, the average duration of ACh-activated elementary currents was less voltage sensitive in comparison with those in freshly dissociated muscle (*see* Table, Fig. 3*A*). This is consistent with a previous report (Mishina et al., 1986; but *see* Cull-Candy et al., 1982*b* for human muscle fibers).

The apparent open time distributions for channels recorded in freshly dissociated and in long-term cultured fibers are shown in Fig. 3*B* and *C*. One exponential curve was found to best fit the histograms obtained in freshly dissociated muscle fibers (Fig. 3*B*), with an average time constant (τ) of 2.0 ± 0.1 msec (n = 9). In experiments on long-term cultured muscle fibers the histograms were best fitted by the sum of two exponentials (Fig. 3*C*) with time constants: τ_1 = 1.5 ± 0.4 and τ_2 = 6.8 ± 0.7 msec (n = 9). It should be considered that the records were performed at a pipette potential of 60 mV, that may represent a more hyperpolarized membrane potential in freshly dissociated muscle fibers, because in freshly dissociated fibers resting potential (judged from the reversal potential of ACh-activated currents) was −67 ± 1 mV (n = 8), which is slightly more negative than in long-term cultured fibers, where it was −55 ± 4 mV (n = 14) (*see also* Lee, Miledi & Ruzzier, 1987).

AChR Density at the Former Endplate

SHORT-TERM EFFECTS

In a previous study (Bloch et al., 1986), collagenase treatment was reported to alter the organization of junctional AChRs immediately after dissociation. This was proposed to be a consequence of the diffusion of junctional AChRs aggregates in extrajunctional areas, where the fluorescence signal became appreciable. On the other hand, Jones and Salpeter (1983) reported that the postsynaptic AChR density was not altered up to 7 hr after collagenase treatment. To investigate the possibility of AChR dispersion in our experimental conditions, we monitored by videomicroscopy the distribution of tetramethylrhodamine-αBTx in identified endplates of living fibers (Fig. 4*A*), during the first few hours following enzymatic dissociation (*see* Materials and Methods). The fluorophore revealed the selective localization of the AChRs at the endplate, which remained apparently unchanged up to 6 hr after dissociation. Analyses of the fluorescence intensity values, carried out in fibers immediately after collagenase digestion and 6 hr later, indicate that the intensity decreased up to 5% with time but was not accompanied by any concomitant increase of the signal in the perijunctional area (Fig. 4*B*). Fluorescence measurements, however, might not be sensitive enough to reveal a low degree of AChR dispersion from the endplate. The distribution of AChRs was, therefore, additionally studied at the molecular level by electron microscopy. Single fibers were chemically fixed and rapidly frozen or processed for immunolocalization one to two hours after dissociation. Freeze-drying and shadowing were performed under high vacuum without previous fracture of the specimen (*see* Materials and Methods). Figure 5*A* shows a replica of the external surface of the plasmalemma where the postsynaptic area is depicted as a folded region featuring a large number of tightly packed protrusions (Grohovaz, Limbrick & Miledi, 1982). The transition from the junctional to the extrajunctional region is evidenced by the flattening of the surface and by the abrupt disappearance of junctional protrusions replaced by a population of very large particles. No class of particles displayed a gra-

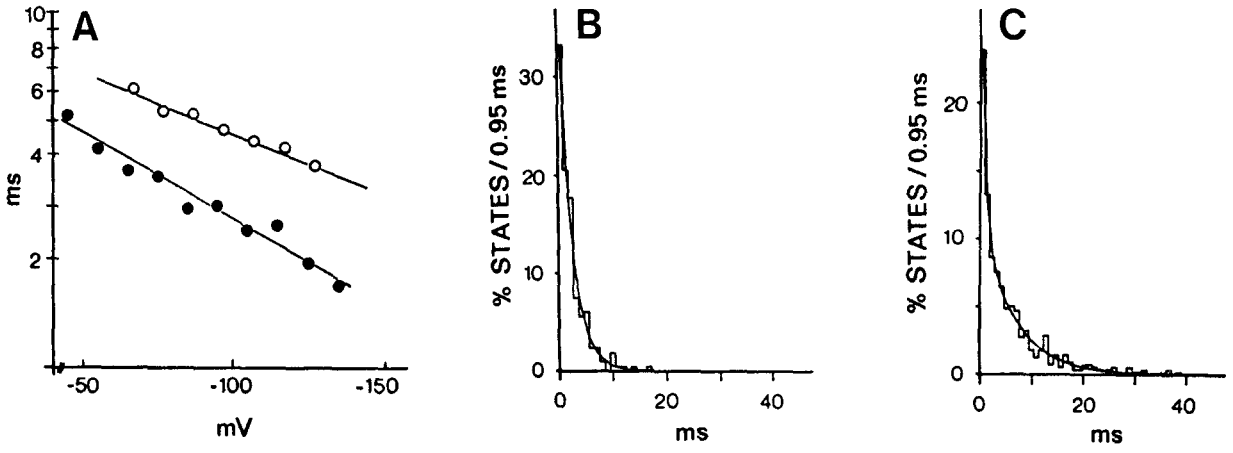

Fig. 3. Kinetic properties of ACh-activated channels. (*A*) Voltage dependence of the average duration (t) of ACh-activated elementary currents in cell-attached patches of freshly dispersed muscle fibers (filled symbols) and muscle fibers kept in culture for nine days (open symbols) in semilogarithmic coordinates. Lines were drawn with parameters by fitting the data to the equation of the form $t_{(V)} = t_o \cdot e^{(-V/H)}$ (*see* Results). Parameters for the two representative experiments are: in freshly dissociated fibers $t_{o1} = 0.85 \pm 0.09$ msec (mean ± SEM), $H_1 = 89.1 \pm 7.1$ mV, and in long-term cultured muscle $t_{o2} = 2.05 \pm 0.11$ msec, H_2 126.0 ± 7.3 mV. (*B*) Representative histograms of elementary current durations in freshly dissociated muscle fibers and (*C*) in muscle fibers cultured for six days. Ordinate represents frequency of elementary events (states) occuring in time intervals of 0.95 msec. In *B*, the curve was drawn by fitting an exponential function to the data where the time constant is 2.4 msec. In *C*, the curve fitted to the histogram is a sum of two exponential functions with time constants of 0.8 and 6.4 msec. In both experiments the pipette potential was 100 mV. However, the potential across the patch may be higher in the freshly denervated muscle as in these cells reversal potential for ACh-activated channels is more negative by about 10 to 20 mV (*see* Results).

Table. Conductance and kinetic properties of AChR-channels

Experimental condition	Conductance (pS) mean ± SD	Apparent channel open time (msec) mean ± SD	Voltage sensitivity (mV) mean ± SEM
Freshly dissoc. fibers (n = 7)	75.1 ± 6.1	1.8 ± 0.6	98.3 ± 17.5
Cultured fibers (n = 9)	48.8 ± 8.6	5.0 ± 0.7	142.0 ± 22.4

Average conductances and mean apparent channel open durations for ACh-activated elementary currents from freshly dissociated muscle fibers and fibers kept in culture for more than 4 days. Channel properties did not change with time in culture. The slope conductances were estimated by linear regression analysis of current-voltage plots of the major conductance class of elementary currents (*see* Fig. 2). The mean elementary current duration was estimated at 40 mV pipette potential. Voltage sensitivity was estimated by fitting the open duration data *vs.* membrane potential to the equation of Magleby and Stevens (1972, *see* Materials and Methods). Membrane potential was assumed to be equal to the driving potential for current through ACh-activated channels, where the reversal potential was determined by linear regression from current-voltage plots as on Fig. 2. (n is number of patches.)

dient of density in the perijunctional region. In agreement with these results, the localization of AChRs by colloidal gold immunolabeling (Fig. 5*B*) showed a distinct border between the crest of junctional folds, where the labeling was densely packed, and the extrajunctional areas, where no immunolabeling was appreciated. Taken together, all these results indicate that the density gradient of AChRs at the border of the junctional area is not diminished immediately after the dissociation of muscle fibers, as already suggested by the discrete localization of autoradiographic and immunofluorescence labeling.

Long-Term Effects

After two to three weeks of *in vivo* denervation, the density of junctional AChRs does not change significantly (Salpeter & Loring, 1985; Shyng & Salpeter, 1989; Fumagalli et al., 1990). However, the

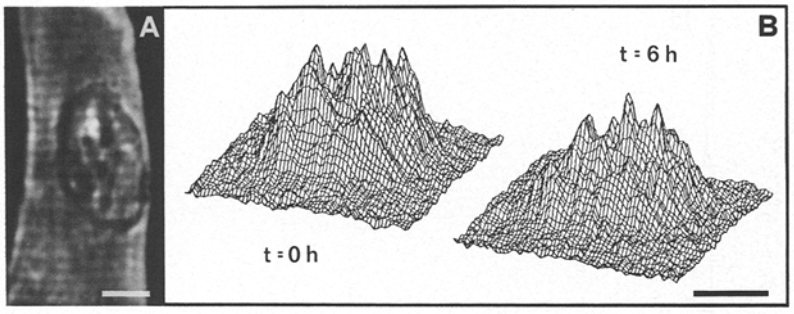

Fig. 4. Localization of ACh receptors in living fibers shortly after dissociation. αBTx-tetramethylrhodamine staining was monitored by low-light videomicroscopy from a dark-field-identified endplate in *A*. *B* represents two plots of the fluorescence intensity, immediately after dissociation and 6 hr later. The intensity significantly diminished at the junctional area but did not increase, concomitantly, in the perijunctional area. Scale bars: 10 μm.

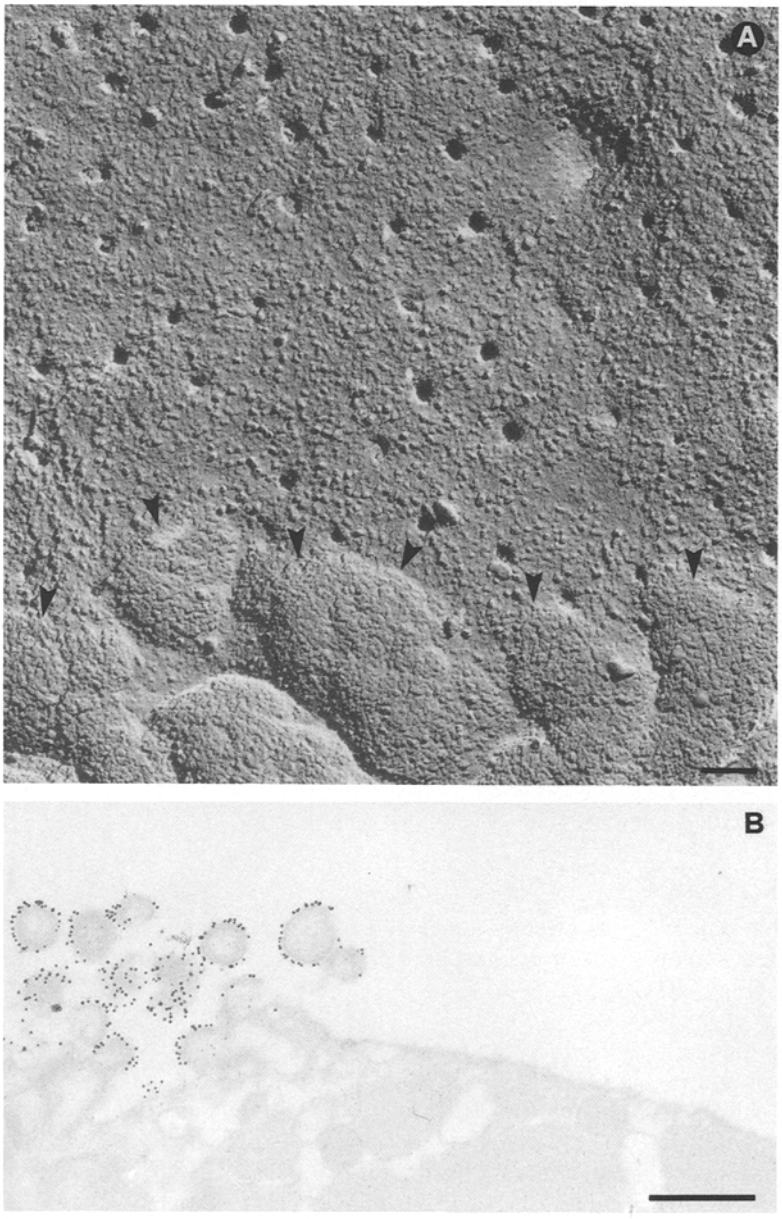

Fig. 5. Ultrastructural appearance of the sarcolemma contiguous with the postsynaptic region. (*A*) Replica of the external surface of a muscle fiber exposed by freeze-drying. After two hour dissociation, the postsynaptic (indicated by arrowheads) and perijunctional regions are still characterized by a folded and flat appearance, respectively. Note that the two regions are further differentiated by the presence of two distinct populations of intramembrane particles with dissimilar size and density. Numerous indentations in the sarcolemma are evident in the perijunctional region. (*B*) Electron micrograph of a thin section immunolabeled for the AChRs by the colloidal gold technique. Two hours after dissociation, AChRs are still densely packed alongside the crest of the postjunctional folds; the flat perijunctional area is completely devoid of labeling. Scale bars: *A*, 0.1 μm; *B*, 0.5 μm.

degradation rate shows a progressive increase with a $t_{1/2}$ change from 8–10 to 1 day. The density of junctional AChRs is therefore maintained by the replacement of degraded AChRs by less stable AChRs on a one-to-one basis (Levitt & Salpeter, 1981; Shyng & Salpeter, 1989). At difference with these results, in our in vitro experimental conditions, the density of junctional AChRs progressively decreased during the culture. To test whether replacement of degraded AChRs is still active after enzymatic denervation, freshly dissociated fibers were incubated in 2 μg/ml αBTx for 3 hr. Under these conditions, AChRs were assumed to be quantitatively saturated since, in a separate set of patch-clamp experiments, ACh-induced currents were completely blocked after one hour exposure to the toxin (*see also* Berg et al., 1972). After five days in culture, the fibers were exposed to [^{125}I]αBTx. Fibers from the controlateral muscle were treated in the same way except that the initial incubation in αBTx was omitted.

The vast majority of the fibers preincubated with the nonradioactive toxin were devoid of silver grains (Fig. 6*A*), and the remaining fibers only displayed patches of grains (Fig. 6*B*) comparable to the extrajunctional aggregates present in the controlateral muscle fibers (Fig. 6*C*). Therefore, the labeling of new AChRs reveals an impairment in the replacement of junctional AChRs five days after dissociation, i.e., at a time when, in our conditions, postdenervation phenomena are fully expressed.

Discussion

The major finding of this work is that enzymatically isolated muscle fibers, when kept in culture, acquire properties similar to those observed after in vivo resection of the nerve (*see also* Bekoff & Betz, 1977). This conclusion is based on the electrophysiological studies and the distribution of αBTx-labeled AChRs. The extrajunctional membrane areas of muscle fibers cultured for more than three days displayed significant density of AChRs. This is in agreement with data obtained on muscle fibers denervated in vivo (Miledi, 1960*a*, *b*; Fambrough, 1979). Interestingly, the appearance of extrajunctional AChRs after enzymatic nerve removal is comparable to that described by Ko, Anderson and Cohen (1977), where random hot spots of AChR accumulation were observed.

The study of single ACh-activated channel properties extends these conclusions. Channel conductance and kinetic properties changed as after in vivo denervation. In fact, we observed a decrease in the conductance of the major amplitude class of elementary current events (from 75 to 48 pS) and, at the same time, an increase of the mean apparent channel open time (from 1.8 to 5.0 msec) (Cull-Candy et al., 1982*b*; Henderson et al., 1987). The presence of two time constants in long-term cultured fibers may reflect two distinct channel kinetic states, which are at least in part due to different channel amplitude classes (Henderson et al., 1987; Mulrine & Ogden, 1989), but it could also reflect different kinetic states of the major conductance state (*reviewed by* Brehm & Henderson, 1988). Due to the low probability of occurrence of the high conductance state of ACh-activated elementary currents, we were not able to resolve this question. In long-term cultured muscle fibers, we resolved at least one subconductance level in ACh-activated elementary currents. The role of these subconductance states is not known; it may be due to the complex structure of the channels (Mishina et al., 1986) and/or to the putative existence of multiple types of subunits (Hartman & Claudio, 1990).

The only aspect of this "in vitro denervation" inconsistent with the results previously described in vivo is the observed decreased density of AChRs at the endplate area. In fact, after in vivo denervation, the total number of AChRs at the endplate was reported to remain unchanged for up to three weeks (Salpeter & Loring, 1985; Fumagalli et al., 1990). For this, the degradation of old junctional AChRs and the local incorporation of new receptors both increased to the same extent (Levitt & Salpeter, 1981; Shyng & Salpeter, 1989). Two possibilities could account for the decreasing density of junctional AChRs observed in our experimental conditions : (i) increased lateral mobility of AChR complexes, due to the enzymatic treatment (Bloch et al., 1986), and (ii) lack of replacement of the degraded junctional AChRs. It should be pointed out that fragmentation of the endplate (Miledi & Slater, 1968) could be responsible for a partial shedding.

If the decrease of junctional AChRs were determined by their dispersion in the surrounding membrane, then the receptor density should exhibit a broad Gaussian distribution (peak in the endplate area) over the perijunctional region. This is clearly not the case, since neither a gradient of intramembrane particles exposed to the surface by freeze-drying, nor a positive immunolocalization of AChRs were observed in the regions bordering with the postsynaptic area. A similar conclusion can be drawn from the experiments where rhodamine-labeled AChRs were followed in living fibers at different times after enzymatic nerve deprivation. Neither dispersion nor redistribution of the fluorescence signal was observed in the first hours after dissociation. Note that according to the first possibility, this pro-

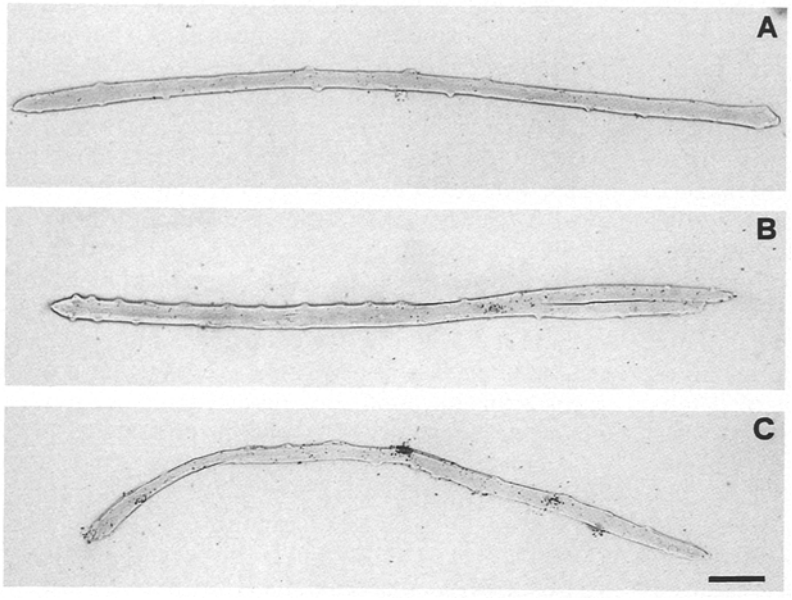

Fig. 6. Autoradiographs showing the distribution of newly inserted AChRs in cultured muscle fibers. Original receptors of fibers *A* and *B* (but not *C*) were saturated with nonradioactive αBTx at the time of enzymatic dissociation. After five days of culture, all the fibers were exposed to [^{125}I]αBTx. Control fibers show the usual dense aggregate of silver grains and, sometimes, additional aggregates along the fiber (*C*). Fibers preincubated with the toxin were generally devoid of silver grain precipitates (*A*), although some (*B*), occasionally, showed patches similar to those observed in the extrajunctional regions of the control (*C*). Scale bar in *C*: 100 μm (*A–C*).

cess would be expected to occur at a high rate. Our data are clearly incompatible with the marked decrease and blurring of AChR fluorescence observed by Bloch and co-workers (1986) in the hours immediately following collagenase treatment. It is unlikely that the enzyme concentration is the responsible factor, since in our experiments the concentration (1–3 mg/ml) was higher than that used in the study by Bloch et al. (1986), where AChR fluorescence changes were observed at concentrations as low as 0.4 mg/ml. The only explanation we can offer is the different toxicity and/or activity of types or batches of collagenase. However, the same batches of collagenase are no longer available and comparison is impossible. On the other hand, when AChRs were saturated by αBTx immediately after dissociation, the incorporation of new receptors was absent or very small at the junctional area in the following days. Our results therefore suggest that the decline in the number of junctional AChRs we observed occurring at a slow rate during the culture period is due to an increased degradation of old receptors coupled to an impaired incorporation of new ones in the former endplate area. This conclusion contrasts with the results obtained in denervated muscles in vivo (Levitt & Salpeter, 1981). Since the dissociation procedure causes the enzymatic digestion of the basal lamina (Betz & Sakmann, 1973; Bekoff & Betz, 1977; Grohovaz et al., 1982; Glavinović, Lee & Miledi, 1987) it is tempting to suggest that the removal of associated proteins, like agrin, involved in the clustering of AChRs (McMahan & Wallace, 1989), might prevent the insertion or trapping of new AChRs in the postsynaptic region.

In conclusion, enzymatic denervation of adult muscle fibers seems to be a useful model for the study of postdenervation changes. In view of the three main hypotheses advanced to account for the expression of postdenervation phenomena, our results seem consistent with the absence of nerve being a sufficient trigger for the full expression of postdenervation changes in cultured muscle fibers. The activity (or rather inactivity; Lømo & Rosenthal, 1972) of muscle fibers in culture cannot fully explain the development of postdenervation changes. In our conditions, we observed (*data not shown*) that cultured muscle fibers were spontaneously active (*see also* Lee et al., 1987). Moreover, nerve breakdown products (Cangiano, 1985) can be ruled out as major triggers of postdenervation phenomena, since muscle fibers were kept in culture medium, which was readily exchanged.

We wish to thank Dr. Jacopo Meldolesi for reading an earlier version of the manuscript. This work was supported by grants from: Consiglio Nazionale delle Ricerche (F.G. and F.R.), Ministero Università, Ricerca Scientifica e Tecnologica, grants 60% and 40% (F.R.), Universities of Trieste, Italy, and Ljubljana, Slovenia, Joint project (F.R. and R.Z.) and Ministry of Science and Technology grant no. P3-0155-381 (R.Z.). F.R. wishes to thank Cassa di Risparmio di Trieste for a generous financial support. Partly supported also by Telethon -Italy.

References

Auerbach, A., Sachs, F. 1984. Patch clamp studies of single ionic channels. *Annu. Rev. Biophys. Bioeng.* **13**:269–302

Axelsson, J., Thesleff, S. 1959. A study of supersensitivity in denervated mammalian skeletal muscle. *J. Physiol.* **147:**178–193.

Bekoff, A., Betz, W.J. 1977. Physiological properties of dissociated muscle fibres obtained from innervated and denervated rat muscle. *J. Physiol.* **271:**25–40

Berg, D.K., Kelly, R.B., Sargent, P.B., Williamson, P., Hall Z.W. 1972. Binding of α-bungarotoxin to acetylcholine receptors in mammalian muscle. *Proc. Natl. Acad. Sci. USA* **69:** 147–151

Betz, W., Sakmann, B. 1973. Effects of proteolytic enzymes on function and structure of frog neuromuscular junction. *J. Physiol.* **230:**673–688

Bloch, R.J., Steinbach, J.H., Merlie, J.P., Heinemann, S. 1986. Collagenase digestion alters the organization and turnover of junctional acetylcholine receptors. *Neurosci. Lett.* **66:**113–119

Brehm, P., Henderson, L. 1988. Regulation of acetylcholine receptor channel function during development of skeletal muscle. *Dev. Biol.* **129:**1–11

Cangiano, A. 1985. Denervation supersensitivity as a model for the neural control of muscle. *Neuroscience* **14:**963–971

Colquhoun, D., Sakmann, B. 1985. Fast events in single-channel currents activated by acetylcholine and its analogues at the frog muscle endplate. *J. Physiol.* **369:**501–557

Corey, D.P., Stevens, C.F. 1983. Science and technology of patch-recording electrodes. *In:* Single-Channel Recording. B. Sakmann and E. Neher, editors, pp. 53–68. Plenum, New York and London

Cull-Candy, S.G., Miledi, R., Uchitel, O.D. 1982*a*. Denervation changes in normal and myasthenia gravis human muscle fibres during organ culture. *J. Physiol.* **333:**227–249

Cull-Candy, S.G., Miledi, R., Uchitel, O.D. 1982*b*. Properties of junctional and extrajunctional acetylcholine-receptors channels in organ cultured human muscle fibres. *J. Physiol.* **333:**251–267.

Dempster, J. 1989. Computer analysis of electrophysiological signals. *In:* Microcomputers in Physiology: A Practical Approach. pp. 53–93. IRL Press, Oxford

Fambrough, D.M. 1979. Control of acetylcholine receptors in skeletal muscle. *Physiol. Rev.* **59:**165–227

Fumagalli, G., Balbi, S., Cangiano, A., Lømo, T. 1990. Regulation of turnover and number of acetylcholine receptors at neuromuscular junctions. *Neuron* **4:**563–569

Glavinović, M.I., Lee, S., Miledi, R. 1987. Effect of collagenase treatment and subsequent culture on rat muscle fiber acetylcholinesterase activity. *J.Neurosci. Res.* **18:**519–524

Grohovaz, F., Limbrick, A.R., Miledi, R. 1982. Acetylcholine receptors at the rat neuromuscular junction as revealed by deep etching. *Proc. R. Soc. London B* **215:**147–154

Gutmann, E. 1976. Neurotrophic relations. *Annu. Rev. Physiol.* **38:**177–217

Hamill, O.P., Marty, A., Neher, E., Sakmann, B., Sigworth, F.J. 1981. Improved patch-clamp techniques for high-resolution current recording from cells and cell-free membrane patches. *Pfluegers Arch.* **391:**85–100

Hamill, O.P., Sakmann, B. 1981. Multiple conductance states of single acetylcholine receptor channels in embryonic muscle cells. *Nature* **294:**462–464

Hartman, D.S., Claudio, T. 1990. Coexpression of two distinct muscle acetylcholine receptor *a*-subunits during development. *Nature* **342:**372–375

Hartzell, H.C., Fambrough, D.M. 1972. Acetylcholine receptors. Distribution and extrajunctional density in rat diaphragm after denervation correlated with acetylcholine sensitivity. *J. Gen. Physiol.* **60:**248–262

Henderson, L.P., Lechleiter, J.D., Brehm, P. 1987. Single channel properties of newly synthesized acetylcholine receptors following denervation of mammalian skeletal muscle. *J. Gen. Physiol.* **89:**999–1014

Henigman, F., Kordaš, M., Zorec, R. 1987. An inexpensive head stage for the 'patch-clamp' apparatus. *J. Physiol.* **391:**11 P

Ito, Y., Miledi, R., Vincent, A., Newsom-Davis, J. 1978. Acetylcholine receptors and endplate electrophysiology in myasthenia gravis. *Brain* **101:**345–368

Jehl, B., Bauer R., Doerge, A., Rick, R. 1981. The use of propane/isopentane mixtures for rapid freezing of biological specimens. *J. Microsc.* **123:**307–309

Jones, S.W., Salpeter, M.M. 1983. Absence of [^{125}I]α-Bungarotoxin binding to motor nerve terminals of frog, lizard and mouse muscle. *J. Neurosci.* **3:**326–331

Ko, P.K., Anderson, M.J., Cohen, M.W. 1977. Denervated skeletal muscle fibres develop discrete patches of high acetylcholine receptor density. *Science* **196:**540–542

Kordaš, M., Zorec, R. 1984. The voltage and temperature dependence of the endplate current in frog skeletal muscle. *Pfluegers Arch.* **401:**408–413

Lee, S., Miledi, R., Ruzzier, F. 1987. The development of tetrodotoxin-resistant action potentials in long-term organ culture of rat muscle. *Q. J. Exp. Physiol.* **72:**601–608

Levitt, T.A., Salpeter, M.M. 1981. Denervated endplates have a dual population of junctional acetylcholine receptors. *Nature* **291:**239–241

Lømo, T., Rosenthal, J. 1972. Control of acetylcholine sensitivity by muscle activity in the rat. *J. Physiol.* **221:**493–513

McArdle, J.J. 1983. Molecular aspects of the trophic influence of nerve on muscle. *Prog. Neurobiol.* **21:**135–198

McMahan, U.J., Wallace, B.G. 1989. Molecules in basal lamina that direct formation of synaptic specializations at neuromuscular junctions. *Dev. Neurosci.* **11:**227–247

Magleby, K.L., Stevens, C.F. 1972. The effect of voltage on the time course of endplate currents. *J. Physiol.* **223:**141–171

Miledi, R. 1960*a*. The acetylcholine sensitivity of frog muscle fibres after complete or partial denervation. *J. Physiol.* **151:**1–23

Miledi, R. 1960*b*. Junctional and extra-junctional acetylcholine receptors in skeletal muscle fibres. *J. Physiol.* **151:**24–30

Miledi, R., Slater, C.R. 1968. Electrophysiology and electron-microscopy of rat neuromuscular junctions after nerve degeneration. *Proc. R. Soc. London B* **169:**289–306

Mishina, M., Takai, T., Imoto, K., Noda, M., Takahashi, T., Numa, S., Methfessel, C., Sakmann, B. 1986. Molecular distinction between fetal and adult forms of muscle acetylcholine receptors. *Nature* **321:**406–411

Mulrine, N., Ogden, D. C. 1989. Activation of ion channels at the rat endplate *in vitro* by acetylcholine at low and physiological temperature. *J. Physiol.* **415:**35 P

Ritchie, A.K., Fambrough, D.M. 1975. Ionic properties of the acetylcholine receptor in cultured rat myotubes. *J. Gen. Physiol.* **65:**751–767

Ruzzier, F., Grohovaz, F. 1986. Basal lamina influence on the phenotypic expression of rat adult muscle fibres. *Neurosci. Lett.* **Suppl. 26:**S 176

Ruzzier, F., Grohovaz, F., Lorenzon, P., Zorec, R. 1991. Properties of acetylcholine receptor channels in isolated skeletal

muscle fibres in culture. *In:* Plasticity of Motoneuronal Connections. A. Wernig, editor. pp. 145–150. Elsevier Science Publishers BV, Amsterdam

Ruzzier, F., Zorec R. 1988. Acetylcholine activated channels in cultured rat muscle fibres acquire denervation-like properties. *Eur. J. Neurosci.* **Suppl. 1:**17.2

Salpeter, M.M., Loring, R.H. 1985. Nicotinic acetylcholine receptors in vertebrate muscle: properties, distribution and neural control. *Prog. Neurobiol.* **25:**297–325

Schuetze, S.M., Role, L.W. 1987. Developmental regulation of nicotinic acetylcholine receptors. *Annu. Rev. Neurosci.* **10:**403–457

Shyng, S.L., Salpeter, M.M. 1989. Degradation rate of acetylcholine receptors inserted into denervated vertebrate neuromuscular junctions. *J. Cell Biol.* **108:**647–651

Steinbach, J.H. 1989. Structural and functional diversity in vertebrate skeletal muscle nicotinic acetylcholine receptors. *Annu. Rev. Physiol.* **51:**353–365